NACA

RESEARCH MEMORANDUM

HIGH-SPEED WIND-TUNNEL TESTS OF A $\frac{1}{16}$-SCALE MODEL OF THE D-558 RESEARCH AIRPLANE

BASIC LONGITUDINAL STABILITY OF THE D-558-1

By

John B. Wright

Langley Memorial Aeronautical Laboratory
Langley Field, Va.

NATIONAL ADVISORY COMMITTEE FOR AERONAUTICS

WASHINGTON

May 12, 1948

NACA RM No. L7K24

NATIONAL ADVISORY COMMITTEE FOR AERONAUTICS

RESEARCH MEMORANDUM

HIGH-SPEED WIND-TUNNEL TESTS OF A $\frac{1}{16}$-SCALE MODEL OF THE D-558 RESEARCH AIRPLANE

BASIC LONGITUDINAL STABILITY OF THE D-558-1

By John B. Wright

SUMMARY

This report contains the results of pitching-moment, lift, and drag measurements with a $\frac{1}{16}$-scale model of the D-558-1, with no nose-inlet flow, with both the tail removed and with the tail at a constant setting. The tests were conducted through a Mach number range up to 0.96 in the Langley 8-foot high-speed tunnel. In order to facilitate the forwarding of this information, only a limited analysis has been made.

It is indicated that the airplane can experience large changes in static longitudinal stability beyond a Mach number of 0.86. At a Mach number of 0.9 there is a tendency for the airplane to become unstable at low lift coefficients followed by large stable tendency at higher speeds. A part of this change in stability is indicated to be destabilizing effects from wing-fuselage characteristics.

INTRODUCTION

The D-558-1 is a research airplane designed to investigate aerodynamic phenomena in the transonic speed range. It is designed to fly at a level-flight Mach number of 0.85 and is powered by a turbojet unit. It has an unswept wing of aspect ratio 4.17 in a low position on the fuselage.

Wind-tunnel tests of a $\frac{1}{16}$-scale model were conducted to high Mach numbers in the Langley 8-foot high-speed tunnel in order to provide preflight information for the pilot to insure against any catastrophic events due to compressibility effects during flight.

This report presents lift, pitching-moment, and drag results obtained from the internal-balance system with a $\frac{1}{16}$-scale model of the D-558-1 with no nose-inlet flow. In order to expedite this information to the NACA flight-test group at Muroc, Calif., to the manufacturer, Douglas Aircraft Company, and to the Navy, Bureau of Aeronautics, this report contains only the results available at the present time with no detailed analysis.

APPARATUS AND TECHNIQUE

The D-558 investigation was conducted in the Langley 8-foot high-speed tunnel which is a single-return closed-throat type. The maximum corrected test Mach number was approximately 0.96 for this investigation. The Reynolds number varied from about 1.0×10^6 to 1.6×10^6.

Model.- An all-metal $\frac{1}{16}$-scale model of the D-558-1 airplane was constructed by the NACA. The general layout is shown by the three-view drawing in figure 1. The geometry and dimensions of the wing and tail are given in table I. The wing-fuselage fillet was designed from the results of a Douglas-Calcit low-speed development program and differs from that used in reference 1. A general comparison of the two fillets is shown in figure 2. Since no inlet flow was simulated, the nose inlet was faired forward to form a solid nose. The fuselage was hollow to allow for the internal balance.

Model support and balance.- The sting-strut support system used in these tests is shown in figure 3. The sting, containing the balance within the fuselage, was attached to the fuselage inside and well forward. The sting diameter is smaller than the inside diameter of the fuselage so that all aerodynamic forces are transmitted through the balance. The sting enlarges smoothly aft of the model to the angle-of-attack coupling, thence to the support strut. In an attempt to avoid choking the tunnel at the strut location at a low test-section Mach number, a liner to constrict the flow was installed in the throat of the tunnel and designed to obtain the highest possible test Mach numbers at the model location.

The balance consisted of strain-gage elements located on the sting and on component parts of the sting so as to measure pitching moment, normal force, and axial force. A transferral of forces to the airplane center of gravity was required because the pitching moment was found at the center of the pitching-moment gage location which is a small distance from the center of gravity. Further, the normal force and axial force had to be reoriented to the lift and drag directions by simple trigonometry.

Because the interference of the sting on the airplane characteristics was included in the forces measured by the internal balance, two types of tare runs were made for several configurations to evaluate this interference. The tare-measuring arrangement is shown in figures 3 and 4. The tare setup incorporated auxiliary tare arms which had 6-percent airfoils, sweptback 30° in forward portions to minimize high-speed interference effects. The arms were attached in the model to an internal balance similar to that used with the sting for the normal runs.

Corrections.- All data were referred to a center-of-gravity location of 25 percent mean aerodynamic chord shown in figure 1. The data were corrected for angle-of-attack changes due to bending of the sting by determining the angle at each test point and interpolating to obtain constant angle of attack. The effect of temperature on the strain gages was determined in static-load and temperature tests. The temperature of the gages was measured during each run and the corresponding corrections found in static tests applied.

The data have all been corrected for the interference of the sting by measuring this effect by the two types of tare runs shown in figure 4. It was found that the sting produced an interference on pitching-moment coefficient which averaged 0.020 over the Mach number and angle-of-attack range. The interference of the sting on lift coefficient was negligible and on the drag coefficient was approximately 0.006.

The data are presented to a corrected Mach number of about 0.96. Choking occurred at the strut at this throat Mach number due to wake effects. However, there was less than 0.01 Mach number difference in the theoretical choking Mach number at the model location and that attained in these tests. The data are unaffected by choke phenomena as the strut is well aft of the model and pressure measurements indicated no irregularities in the velocity field in the model region at this Mach number.

Corrections for blockage and other wall-interference effects have been applied to these data in a manner similar to that indicated in reference 1. Below a Mach number of 0.9, the corrections to Mach number, to dynamic pressure, and to various coefficients are negligible. Above a Mach number of 0.9, the lift vortex interference is negligible. The total magnitude of the model and wake blockage corrections to Mach number and dynamic pressure are of the same order of magnitude. Typical Mach number corrections are shown as follows:

Test Mach number	Corrected Mach number
0.90	0.905
.925	.933
.94	.96

[redacted]

RESULTS AND DISCUSSION

Complete Model

Figure 5 presents the variation of pitching-moment coefficient and lift coefficient with Mach number for constant angles of attack for the model with a stabilizer incidence $i_t = 2.2^\circ$ and elevator angle $\delta_e = 0^\circ$. Figure 6 shows the variation of drag coefficient with Mach number for the same configuration. In figure 7, the data of figure 5 have been cross-plotted to obtain the variation of pitching-moment coefficient with lift coefficient for various Mach numbers. The static-longitudinal-stability parameter $\partial C_M/\partial C_L$ is shown in figure 8 as a function of Mach number. The slope $\partial C_M/\partial C_L$ was obtained from figure 7 at each Mach number for the two values of lift coefficient required for level flight at sea level and 35,000 feet altitude shown in figure 9. The wing loading was assumed to be 58 pounds per square foot, the design loading of the D-558-1 with about 90 percent of the flight run completed. The values of the lift coefficient at $C_M = 0$ from figure 7 are presented for this tail setting in figure 10 as a function of Mach number.

The static-longitudinal-stability parameter of this airplane, as shown in figures 7 and 8, for this one untrimmed setting remains fairly constant with increasing Mach number up to a Mach number of about 0.86. Around a Mach number of 0.90, a positive slope indicates a possible unstable region in the low lift range which may lead to difficulties in flight. Around a Mach number of 0.93, the unstable range disappears, followed by very large increases in stability through the highest test speed. It is indicated that the large changes in stability can be avoided at high speeds by flight at high altitudes (fig. 8) or increased weight to increase level-flight lift coefficients. In addition, maneuvers which decrease the lift coefficient below that for level flight in this speed range should be avoided.

Tail Off

Figure 11 shows the variation of lift coefficient and pitching-moment coefficient with Mach number for constant angles of attack for the model without the horizontal tail. Figure 11 has been cross-plotted to show in figure 12 the variation of pitching-moment coefficient with lift coefficient for several Mach numbers for the model without the horizontal tail. The tests with horizontal tail off indicate a large positive (destabilizing) increase in $\partial C_M/\partial C_L$ around a Mach number of 0.90 in

the low lift-coefficient range. This behavior reverses at higher Mach numbers to show a negative (stabilizing) value of $\partial C_M / \partial C_L$.

The pitching-moment increment ΔC_M due to the tail was determined from the difference in pitching-moment coefficients for the horizontal tail on and off. The increment ΔC_M chosen at the lift coefficients required for level flight at two altitude conditions at each Mach number is shown in figure 13 as a function of Mach number. This untrimmed tail load also changes abruptly in the high Mach number range.

CONCLUDING REMARK

From tests of a $\frac{1}{16}$-scale model of the D-558-1 airplane with no nose-inlet flow at a constant tail setting, it is indicated that the airplane can experience large changes in static longitudinal stability beyond a Mach number of about 0.86. At a Mach number of approximately 0.9 there is a tendency for the airplane to become unstable at low lift coefficients followed by a large stable tendency at higher speeds. A part of this change in stability is indicated to be destabilizing effects from wing-fuselage characteristics.

Langley Memorial Aeronautical Laboratory
National Advisory Committee for Aeronautics
Langley Field, Va.

REFERENCE

1. Wright, John B., and Loving, Donald L.: High-Speed Wind-Tunnel Tests of a 1/16-Scale Model of the D-558 Research Airplane. Lift and Drag Characteristics of the D-558-1 and Various Wing and Tail Configuration. NACA RM No. L6J09, 1946.

[redacted]

TABLE I

WING AND TAIL DIMENSIONS OF $\frac{1}{16}$-SCALE D-558-1 MODEL

Wing section	NACA 65-110
Wing aspect ratio	4.17
Wing taper ratio	0.54
Wing span, in.	18.76
Wing area, sq ft	0.587
Wing mean aerodynamic chord, in.	4.656
Wing incidence angle, deg	2.0
Wing dihedral, deg	4.0
Wing sweep angle (50-percent chord), deg	0
Wing root chord, in.	5.88
Wing tip chord, in.	3.17
Longitudinal location of 25-percent-mean-aerodynamic-chord point from nose-inlet station, in. (also center-of-gravity location)	11.96
Tail section	NACA 65-008
Tail aspect ratio	4.17
Tail taper ratio	0.55
Tail span, in.	9.18
Tail area, sq ft	0.140
Tail dihedral, deg	0
Elevator area, percent of tail area	25

NATIONAL ADVISORY
COMMITTEE FOR AERONAUTICS

[redacted]

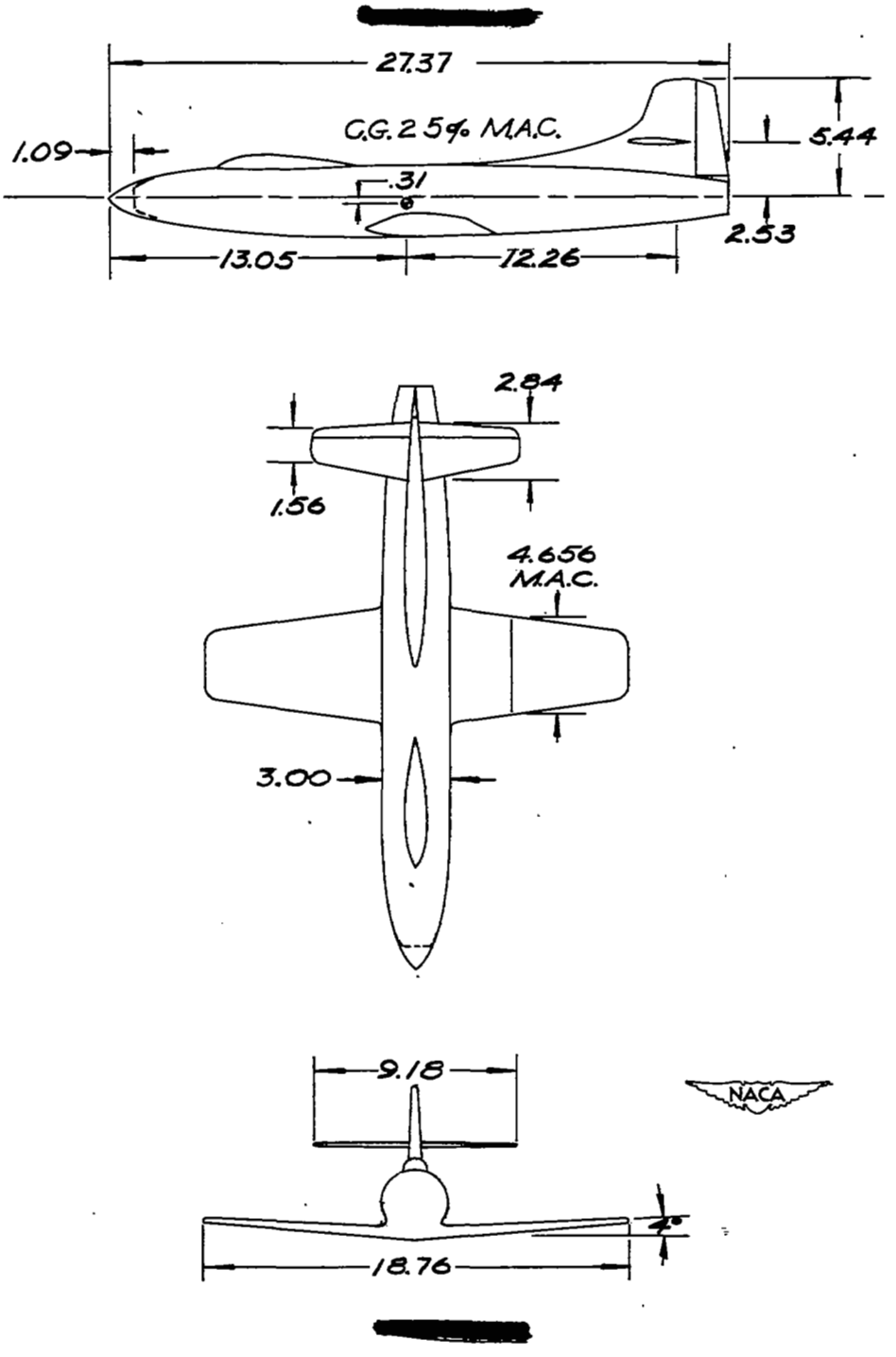

Figure 1.— Drawing of 1/16-scale D-558-1 model as tested in the Langley 8-foot high-speed tunnel. All dimensions in inches.

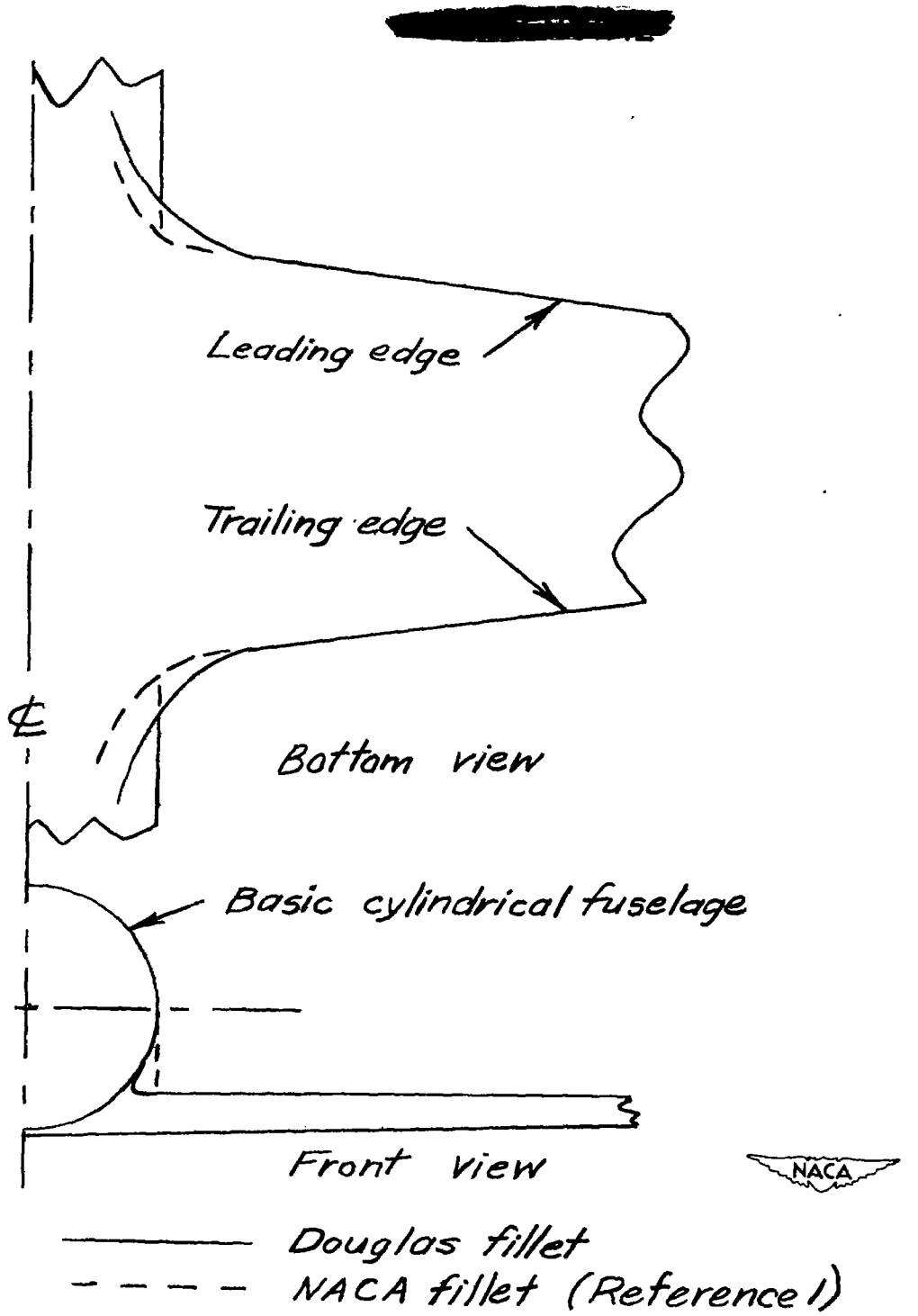

Figure 2.- Approximate comparison of the Douglas and NACA wing fillets.

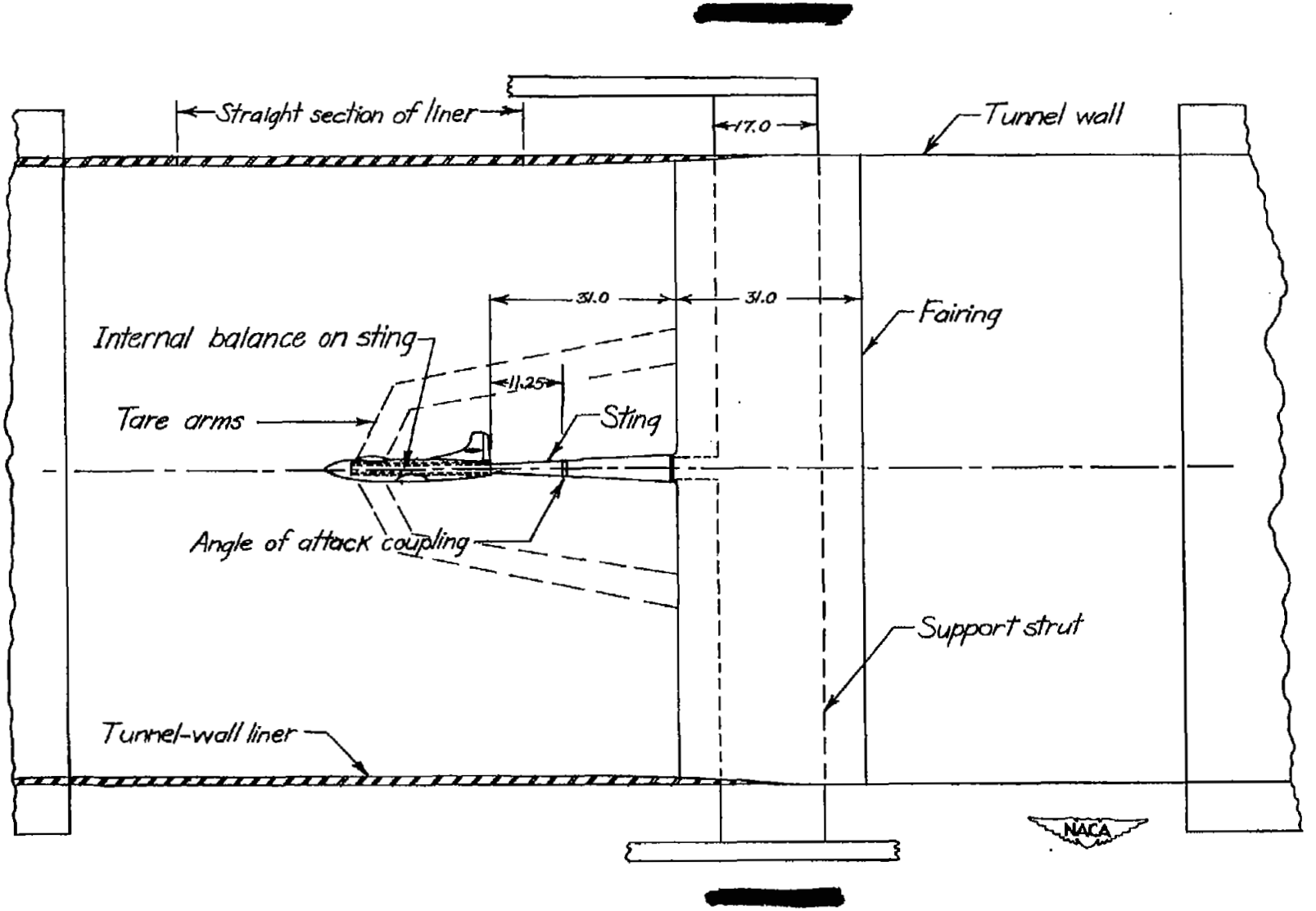

Figure 3.- Model on sting support in the Langley 8-foot high-speed tunnel. All dimensions in inches.

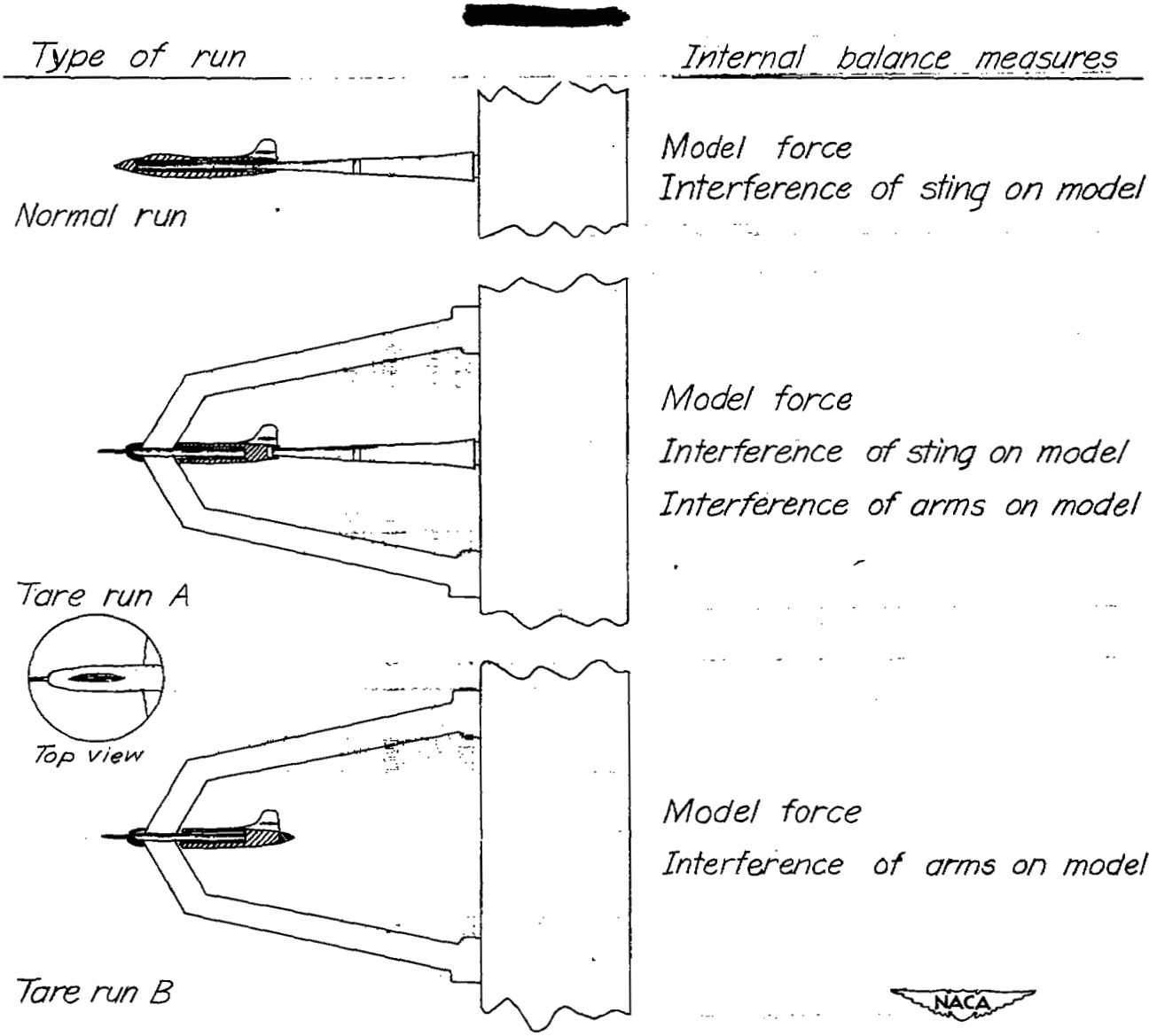

Tare run A – Tare run B = Interference of sting on model

Normal run – (A-B) = Model force

Figure 4.—Model setups and tare evaluation technique.

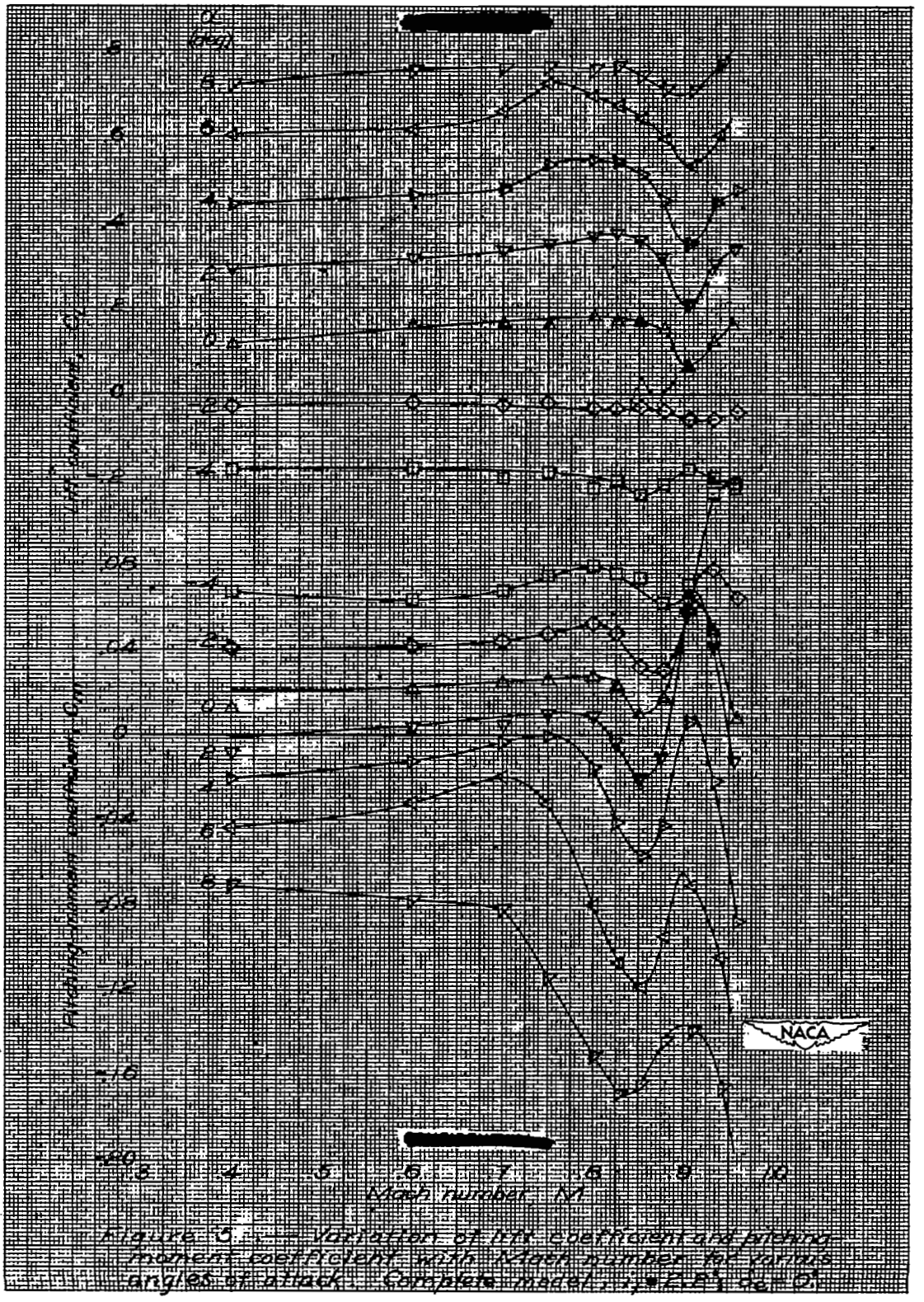

Figure 5.- Variation of lift coefficient and pitching-moment coefficient with Mach number for various angles of attack. Complete model; $i_t = 0°$; $\delta_e = 0°$.

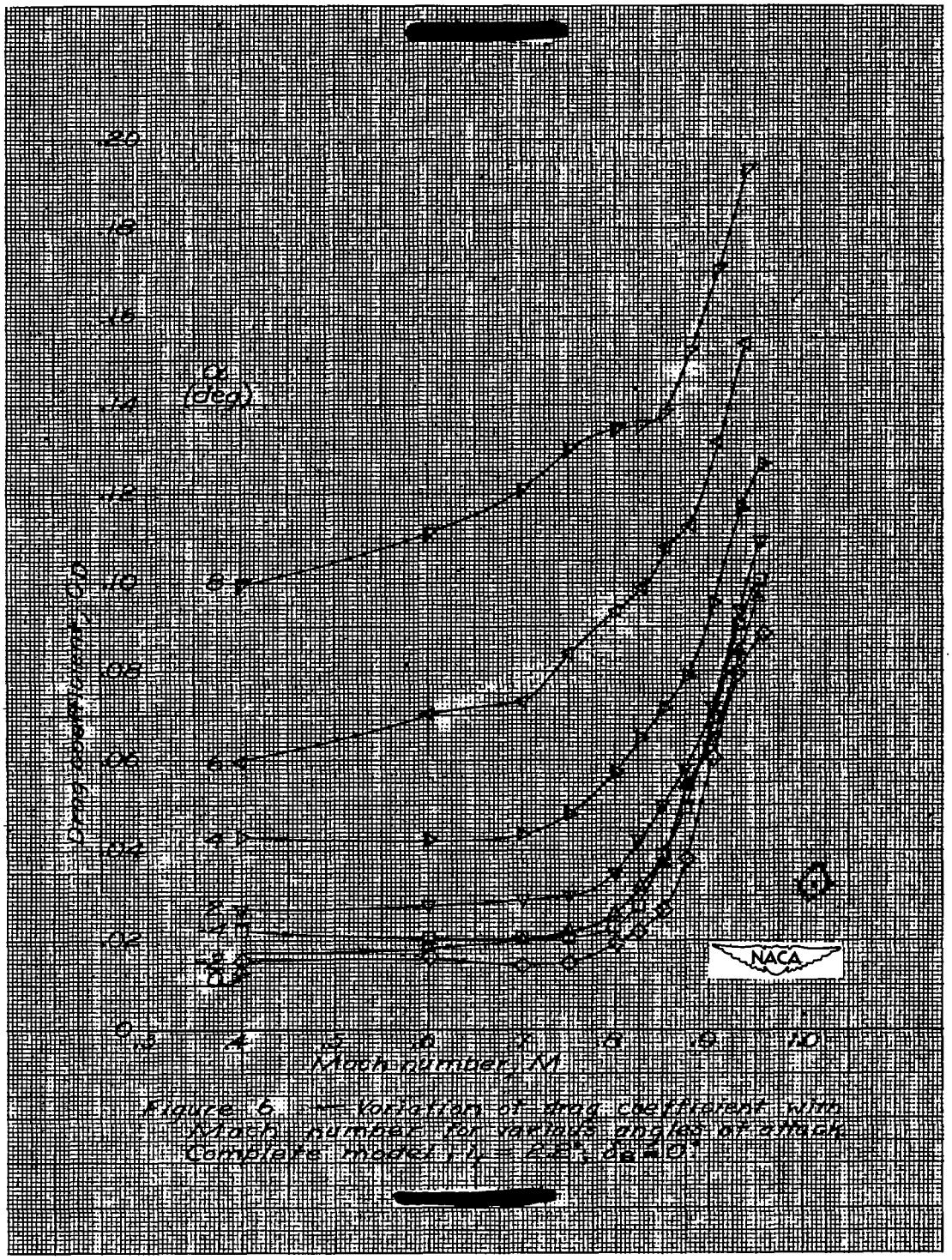

Figure 6. — Variation of drag coefficient with Mach number for various angles of attack. Complete model; $i_t = 2.2°$, $\delta_e = 0°$.

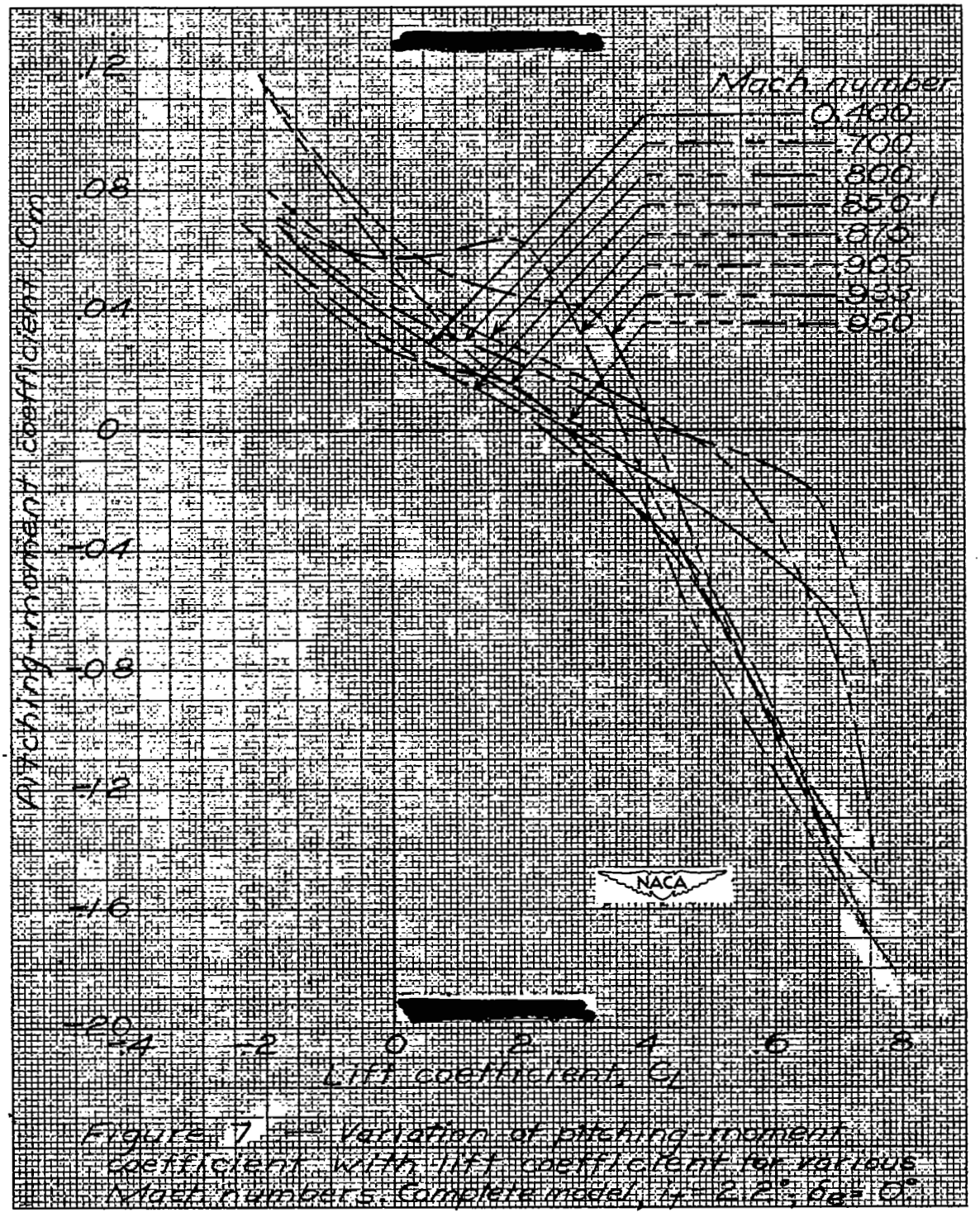

Figure 17.— Variation of pitching moment coefficient with lift coefficient for various Mach numbers. Complete model; $i_t = 2.2°$; $\delta_e = 0°$.

[redacted]

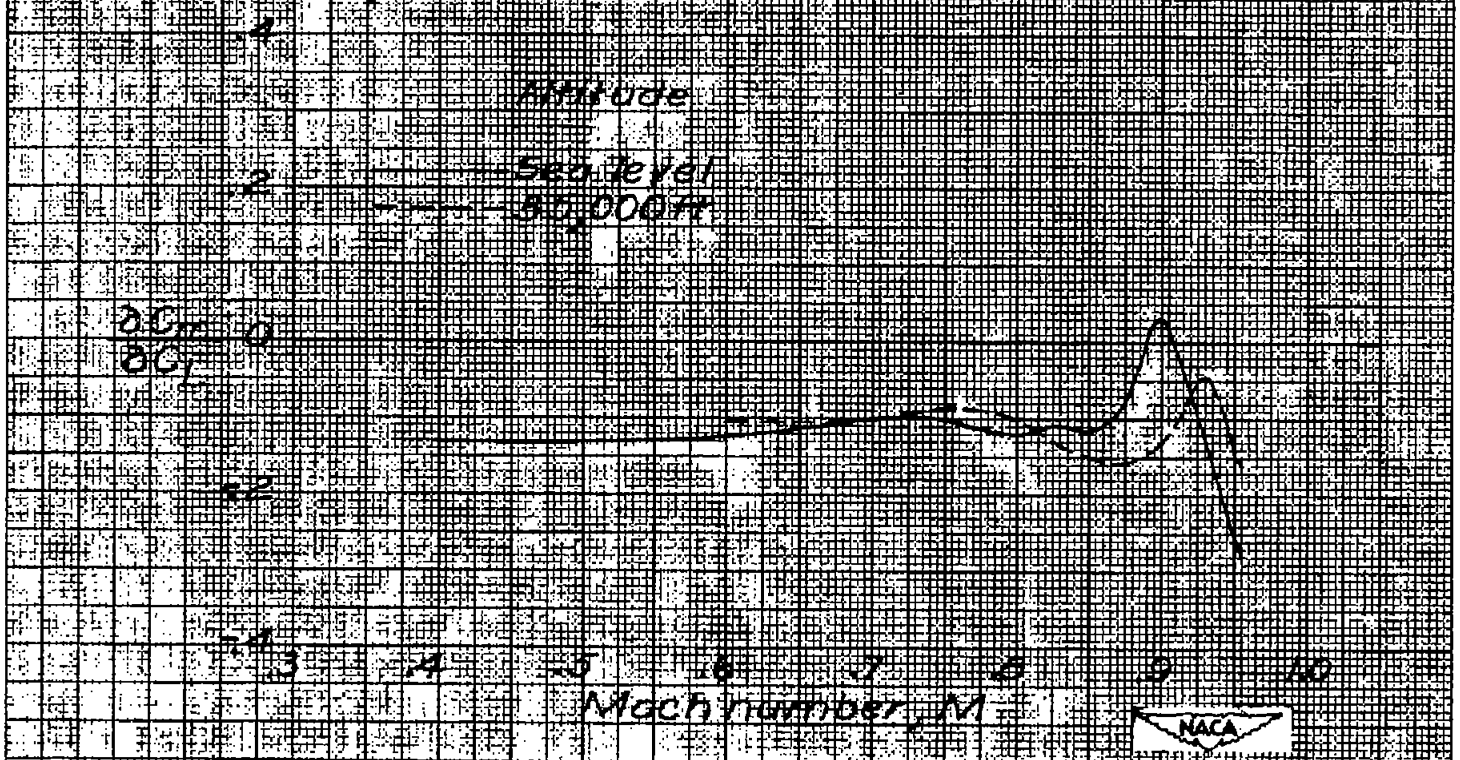

Figure 8.— Variation of the static-longitudinal-stability parameter, $\frac{\partial C_m}{\partial C_L}$, with Mach number for two altitude conditions. Complete model, $i_t = 2.2^\circ$; $\delta_e = 0^\circ$.

[redacted]

[redacted]

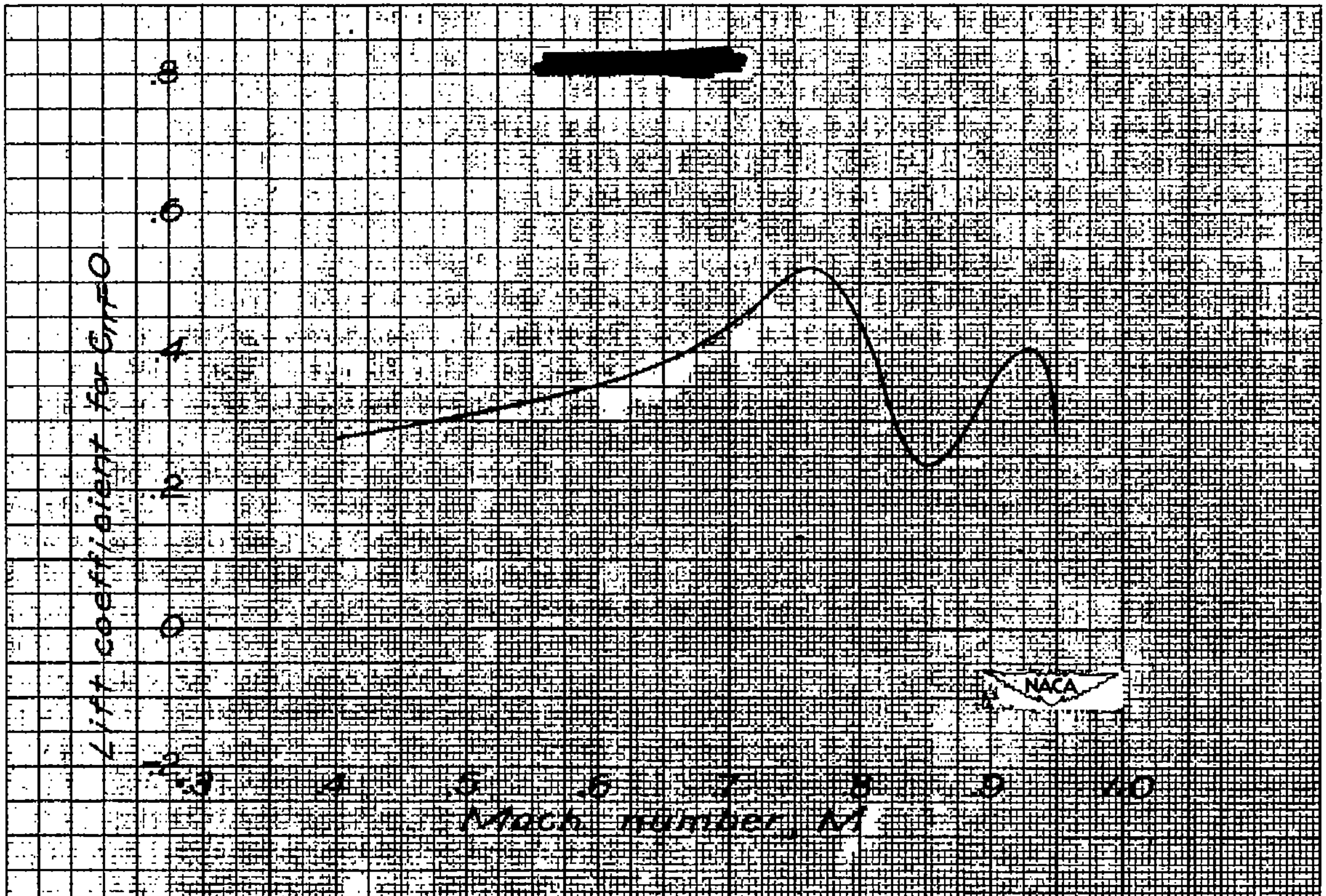

Figure 10.— Variation of lift coefficient for $C_m = 0$ with Mach number. Complete model, $i_t = 2.2°$, $\delta_e = 0°$.

[redacted]

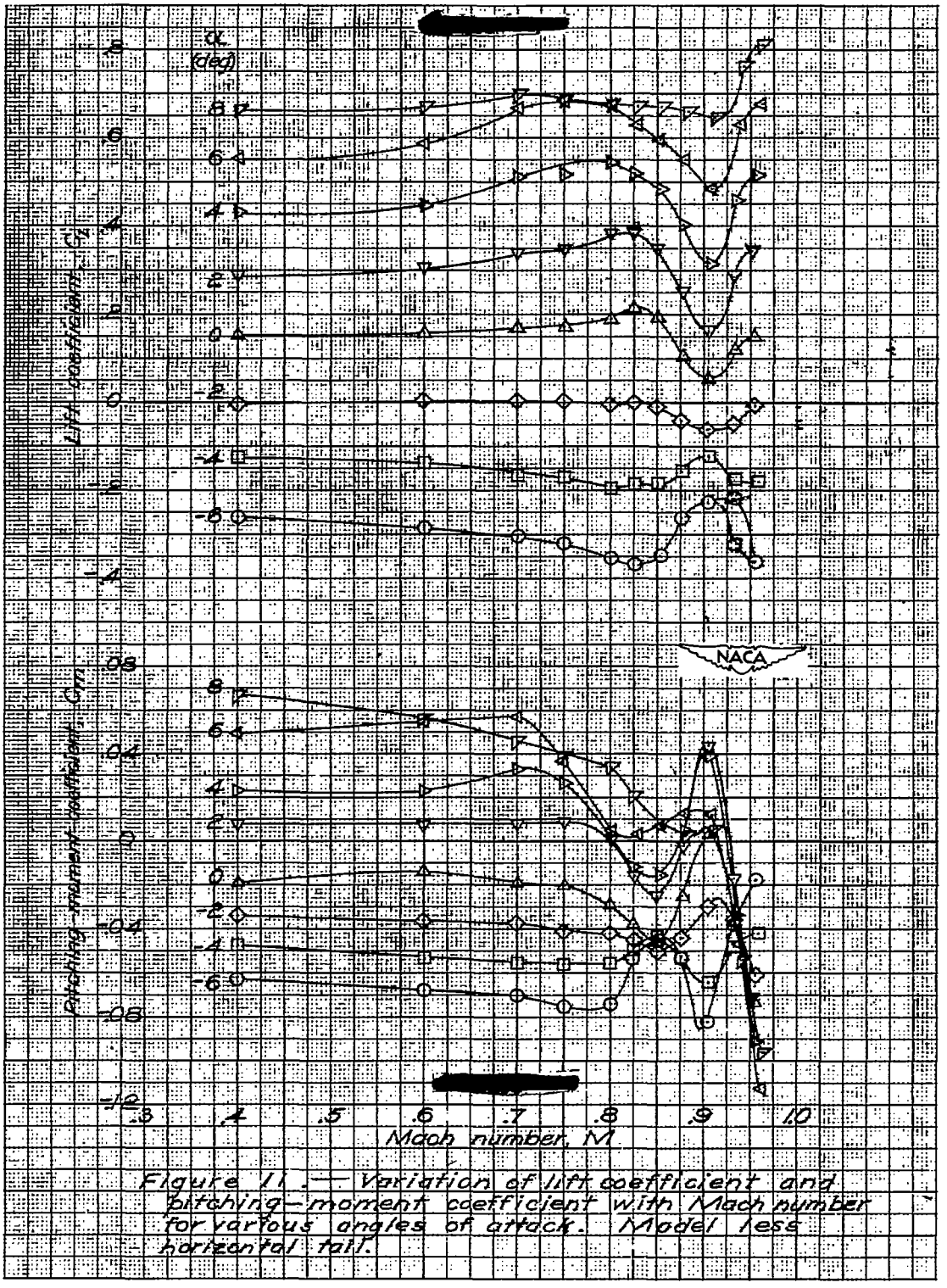

Figure 11. — Variation of lift coefficient and pitching-moment coefficient with Mach number for various angles of attack. Model less horizontal tail.

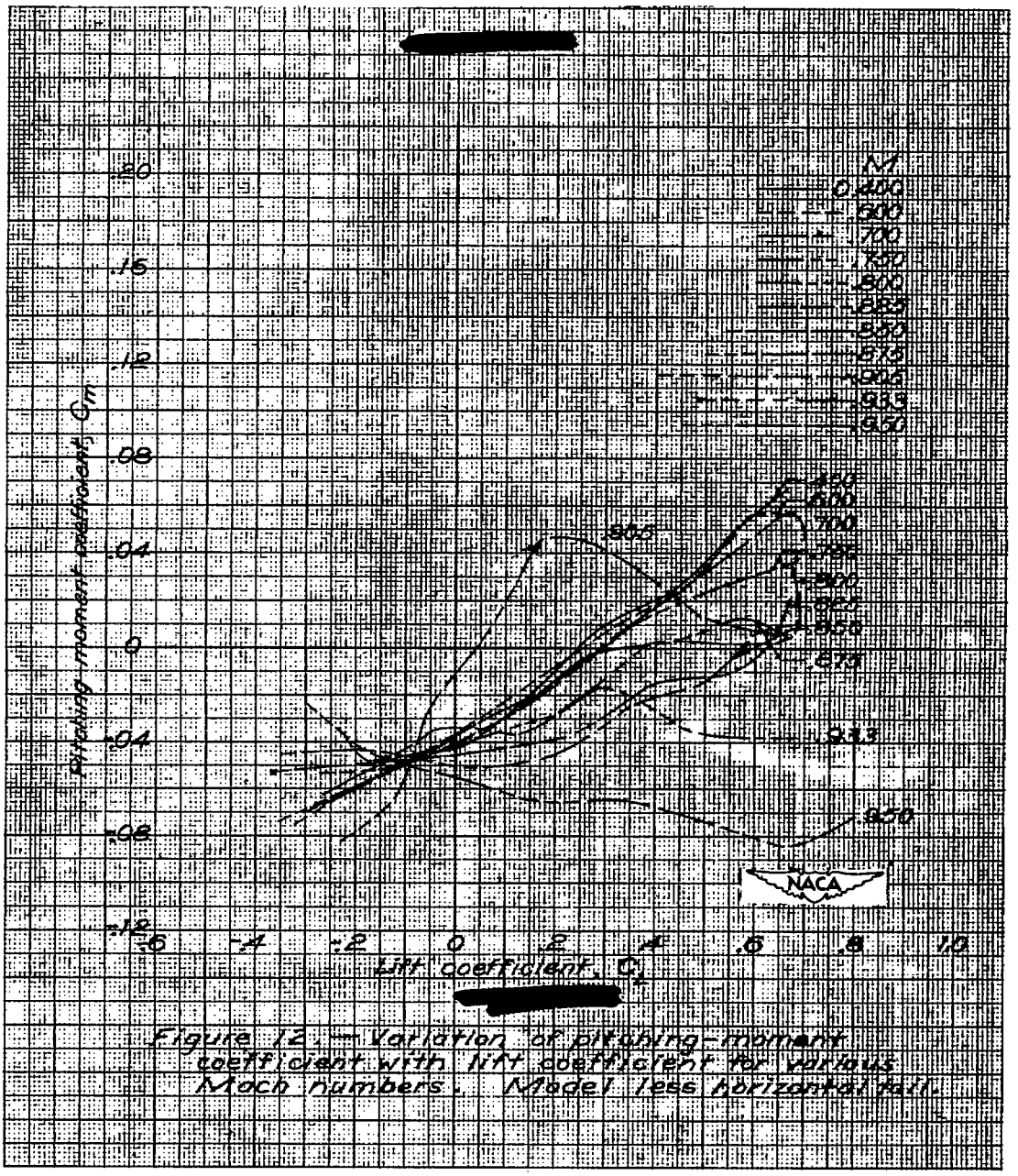

Figure 12.—Variation of pitching-moment coefficient with lift coefficient for various Mach numbers. Model less horizontal tail.

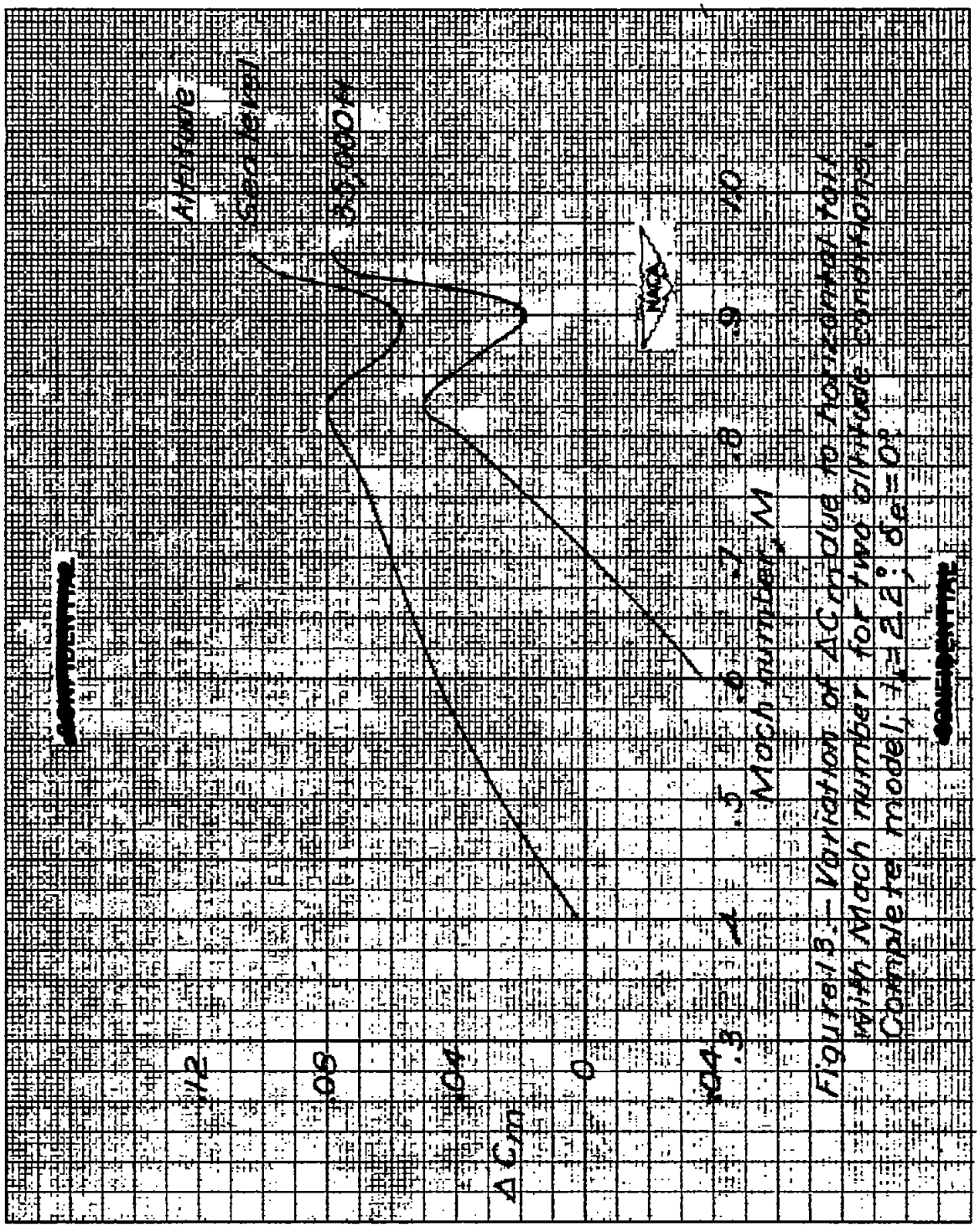

Figure 13.- Variation of $\Delta C_{m_{cg}}$ due to horizontal tail with Mach number for two angles of attack. Complete model; $i_t = 2.2°$; $\delta_e = 0°$.